Journal of Mining and Environment (JME) Vol. 16, No. 1, 2025, 291-306

Shahrood University of Technology

Journal of Mining and Environment (JME)

Journal homepage: www.jme.shahroodut.ac.ir

Iranian Society of Mining Engineering (IRSME)

Participation of Analytical Parameters in Predictive Empirical Models for Rock Mass Deformation Modulus: A Review

Mohammad Reza Shahverdiloo*,and Shokrollah Zare

Faculty of Mining, Petroleum & Geophysics Engineering, Shahrood University of Technology, Shahrood, Iran

Article Info

Received 9 March 2024

Received in Revised form 10 May 2024

Accepted 10 June 2024

Published online 10 June 2024

DOI: 10.22044/jme.2024.14299.2671

Keywords

Deformation modulus

Analytical parameters

In-situ stress

Joint stiffness

Geological strength index

Abstract

The deformation modulus of rock mass is necessary for stability analysis of rock structures, which is generally estimated by empirical models with one to five input parameters/indexes. However, appropriate input parameter participation to establish a sound basis for a reliable prediction has been a challenging task. In this study, the concept of the principal input parameters was developed based on an analytical method with an emphasis on in-situ stress. Based on analytical methods, Young's modulus of intact rock, the joint's shear and normal stiffness, joint set spacing, and in-situ stress are introduced as the main principal input parameters. A review of seventy empirical models revealed that most of them suffered from a lack of analytical parameters. Due to considering practical issues, the geological strength index (GSI) is replaced with joint set spacing; moreover, the in-situ stress effect is perceived by combining Young's modulus and joint stiffness with specific confining pressure and normal stress, respectively. The integration of the analytical base input parameters and practical issues enhanced the reliability of empirical models due to the reasonable prediction of the deformation modulus to numerical or analytical deformability analysis.

1. Introduction

The rock mass deformation modulus (D_f) is a vital and indispensable input parameter to the design and stability analysis of rock structures such as shafts, tunnels, underground caverns, well bores, and dams. D_f is a mechanical parameter that represents the deformation behaviour derived from the applied stress and measured strain and includes the elastic and inelastic values of an in-situ rock mass [1]. Generally, the best methods to determine rock mass deformation behaviour are in-situ tests such as the plate load test and flat jack test [2], dilatometer test, and pressure–meter test [3, 4], and borehole jack test [5]. Ordinarily, the tests above are time–consuming, capital–intensive, and often difficult to perform [6, 7]. The project limitations in terms of cost and time are the underlying causes of persuasion to develop empirical models that are categorised as an indirect approach to estimating D_f. The main steps in developing an empirical model consist of the input parameter selection, analyzing approach, and control and validation. However, there is a lack of consensus among rock engineers due to the diverse range of estimated D_f by different empirical models [8]. It seems the appropriate selection of input parameters has a main role in creating a strong consensus on the prevailing view on empirical models. Over the past decades, numerous empirical models with one to five input parameters/indices have been presented [9, 10, 11, 12, 8, 13, 14, 15, 16]; however, the permutation of parameters involved in empirical models is prominent. It sounds like the simplicity and accessibility of factors are the main bases for inferring the majority of earlier empirical models. In chronological order, Rock Quality Designation index (RQD), Rock Mass Rating (RMR), Rock Tunnelling Quality Index (Q), Rock Mass Index (RMI), and Geological strength index (GSI) are the main rock mass classification systems with a

* Corresponding author: mr.shahverdiloo@shahroodut.ac.ir (M.R. Shahverdiloo)

contribution of geological characteristics included in empirical models, and collectively known as rock characteristics statistically influenced D_f. Although the input parameters have a statistical influence, the empirical models are susceptible to unacceptability due to a relative lack of conceptual parameters. However, the reliability of empirical models parallel involving principal parameters has an analytical background that is rich in data sets.

The analytical method is an indirect approach to estimating D_f that is established based on the equivalent continuum concept for jointed rock masses. The main principle followed by the mentioned approach is the similarity of deformation; in other words, the sum of the intact rock and discontinuity deformations is equal to the deformation of the rock mass equivalent continuum. Duncan and Goodman [17] perceived the rock mass with zero-thickness discontinuities whose deformability is described in terms of shear (k_s) and normal (k_n) stiffness. The load-deformation behaviour of composite materials is the base of their derivation. The methodology of Duncan and Goodman [17] was utilized later in other studies; Kulhawy [18] and Chen [19] considered three orthogonal discontinuity sets, and Amadei [20], Amadei and Savage [21], and Huang et al. [22] perceived non-orthogonal discontinuity sets within rock masses. Fossum [23] derived the expressions for estimating the deformability of rock masses containing randomly distributed discontinuities by using the averaging procedure for fiber composites. Gerrard [24] used the orthorhombic layer theory, which derived elastic models of rock masses containing one, two, or three joint sets with a given thickness. Furthermore, a method was developed for considering non-persistent discontinuities for estimating the deformability of rock masses by Oda [25] and Kulatilake et al. [26]. Based on the mentioned analytical models, Young's modulus of intact rock, the joint's shear and normal stiffness, the joint geometry parameters, joint density (spacing), orientation (dip and dip directions), size and number of joint sets, Poisson's ratio of intact rock, and the joint dilatancy factor are the participated parameters in predicting the D_f. Furthermore, the in-situ stress status has an indisputable role in D_f [27, 28, 29 11, 2, 30, 31] because rock mass mainly constitutes intact rock and joint sets. In addition, Shahverdiloo and Zare [34, 14] mentioned Young's modulus of intact rock depends on confining stress, and the joint's shear and normal stiffness rely on normal stress on a joint plan. Therefore, in-situ stress should be considered in an empirical model to predict deformation modulus [32, 33].

In this study, based on the analytical method, five principal input parameters (PIPs) are introduced for empirical models while considering practical issues. Moreover, to consider the geometry, density, orientation, size, and number of joint set parameters, Ván and Vásárhelyi [35] proposed that GSI be used instead of joint spacing. In addition, the participation of PIPs was comprehensively reviewed in seventy earlier empirical models. Furthermore, based on the authors' studies, Shahverdiloo and Zare [34, 14], proposed that the in-situ stress effect on deformation modulus is considered indirectly by involving confined Young's modulus and scaled joint stiffness in future empirical models.

2. Methodology

The deformation properties of intact rock and discontinuity obtained by the laboratory or in-situ test need to be used in all indirect methods [16]. Duncan and Goodman [17] and Goodman [36] introduced the concept of "equivalent" continuous material, which is the basis of analytical methods to introduce the principal influential parameters in D_f, having the same deformation characteristics (u) as the jointed rock mass. However, the joint set pattern and the derivation method are the main differences between the diverse models (Table 1).

Table 1. Analytical models to predict deformation, shear, or bulk modulus.

	Reference	Deformation modulus	Shear / Bulk modulus	Discontinuity set
1	Duncan and Goodman [17]	$\frac{1}{E_n}=\frac{1}{E}+\frac{1}{k_nS}$	$\frac{1}{G_{nt}}=\frac{1}{G}+\frac{1}{k_sS}$	A horizontal discontinuity sets
	Kulhawy [18]	$E_{mi}=\frac{1}{\frac{1}{E_r}+\frac{1}{k_{ni}S_i}}$	$G_{mij}=\frac{1}{\frac{1}{G_r}+\frac{1}{k_{si}S_i}+\frac{1}{k_{sj}S_j}}$	Three orthogonal
3	Fossum [23]	$E_m=\frac{9K_mG_m}{3K_m+G_m}$	$K_m=\frac{E_r}{9}\left[\frac{3(1+\vartheta_r)Sk_n2E_r}{(1+\vartheta_r)(1-2\vartheta_r)Sk_n+(1-\vartheta_r)E_r}\right]$ $G_m=\frac{E_r}{30(1+\vartheta_r)}\left[\frac{9(1+\vartheta_r)(1-2\vartheta_r)Sk_n+(7-5\vartheta_r)E_r}{(1+\vartheta_r)(1-2\vartheta_r)Sk_n+(1-\vartheta_r)E_r}\right]+\frac{2}{5}\left[\frac{E_rSk_s}{2(1+\vartheta_r)Sk_s+E_r}\right]$	Randomly oriented discontinuities
4	Huang et al. [22]	$\frac{1}{E_x}=\frac{1}{E_r}+\frac{1}{k_{n3}S_3}$	$\frac{1}{G_{xy}}=\frac{1}{G_r}+\frac{1}{k_{s3}S}+\frac{2\sin\theta\cos^2(\theta/2)}{k_sS}$	In three intersections, the angle between the first two sets of joints is θ with the same joint stiffness; index 3 denoted the third joint set.
		$\frac{1}{E_y}=\frac{1}{E_r}+2\sin^2(\theta/2)\left[\frac{\cos^2(\theta/2)k_n+\sin^2(\theta/2)k_s}{k_nk_sS}\right]$	$\frac{1}{G_{yz}}=\frac{1}{G_r}+\frac{2\sin^2\theta\,(k_n+k_s)}{k_sk_nS}$	
		$\frac{1}{E_z}=\frac{1}{E_r}+2\sin^2(\theta/2)\left[\frac{\cos^2(\theta/2)k_n+\sin^2(\theta/2)k_s}{k_nk_sS}\right]$	$\frac{1}{G_{zx}}=\frac{1}{G_r}+\frac{1}{k_{s3}S}+\frac{2\sin\theta\,\sin^2(\theta/2)}{k_sS}$	
5	Zhang [16]	$E_m=\frac{1}{\frac{1}{E_r}+\frac{1}{3}\left[\frac{21}{32k_nS}+\frac{11}{32k_sS}\right]}$	$G_m=\frac{1}{\frac{1}{G_r}+\frac{1}{3}\left[\frac{11}{32k_nS}+\frac{21}{32k_sS}\right]}$	Several discontinuity sets

E_m: Deformation modulus; $E_{x,y,z}$: Deformation modulus in x, y, z direction; E_n and G_{nt} is the elasticity and shear modulus of deformation of equivalent continuous material, respectively; G_m: Shear modulus; E, E_r: The intact rock elasticity modulus; G, G_r: The intact rock shear modulus; K_m: Bulk modulus; k_{ni} and $k_{si}$are the normal stiffness and shear stiffness of the joints for the joint set i, respectively; i (x, y, z), j (y, z, x), and k (z, x, y); the axes n and t are normal and parallel to the joints and therefore in the principal symmetry directions of the rock mass; s or S: The average discontinuity spacing, for all the discontinuity sets; si is the average joint spacing for the joint set i; ϑ_r or ν: Poisson's ratio of intact rock.

The rock mass equivalent elastic continuum is a representative that regularly crosses with a single set of joints (Figure 1), therefore, $u_{\text{jointed rock mass}}=u_{\text{equivalent elastic continuum}}$.
Deformability concepts for a unique compressive (σ) or shear (τ) stress are shown in Figures 1-a and 1-b, respectively. In general, where the applied stress is a combination of compressive and shear stresses, the deformability of a jointed rock mass can be considered as Equation (1) based on the principle of superposition; in other words, D_f can be considered as a combination of elasticity and shear modulus of an equivalent continuous material, which is defined by:

$$D_f = \alpha G_{nt} + \beta E_n \quad (1)$$

where α and β are constant; $\alpha+\beta=1$ and $0\leq\alpha$ & $\beta\leq 1$. Therefore, the mathematical relationship to estimating D_f should be a function of the influential factors on E_n and G_{nt}. Therefore, the deformation modulus of a jointed rock mass should be a combination of parameters that participated in Duncan and Goodman's model, which can be expressed as follows:

$$D_f = f(G_{nt}, E_n) = f(E, G, k_s, k_n, S) \quad (2\text{-a})$$

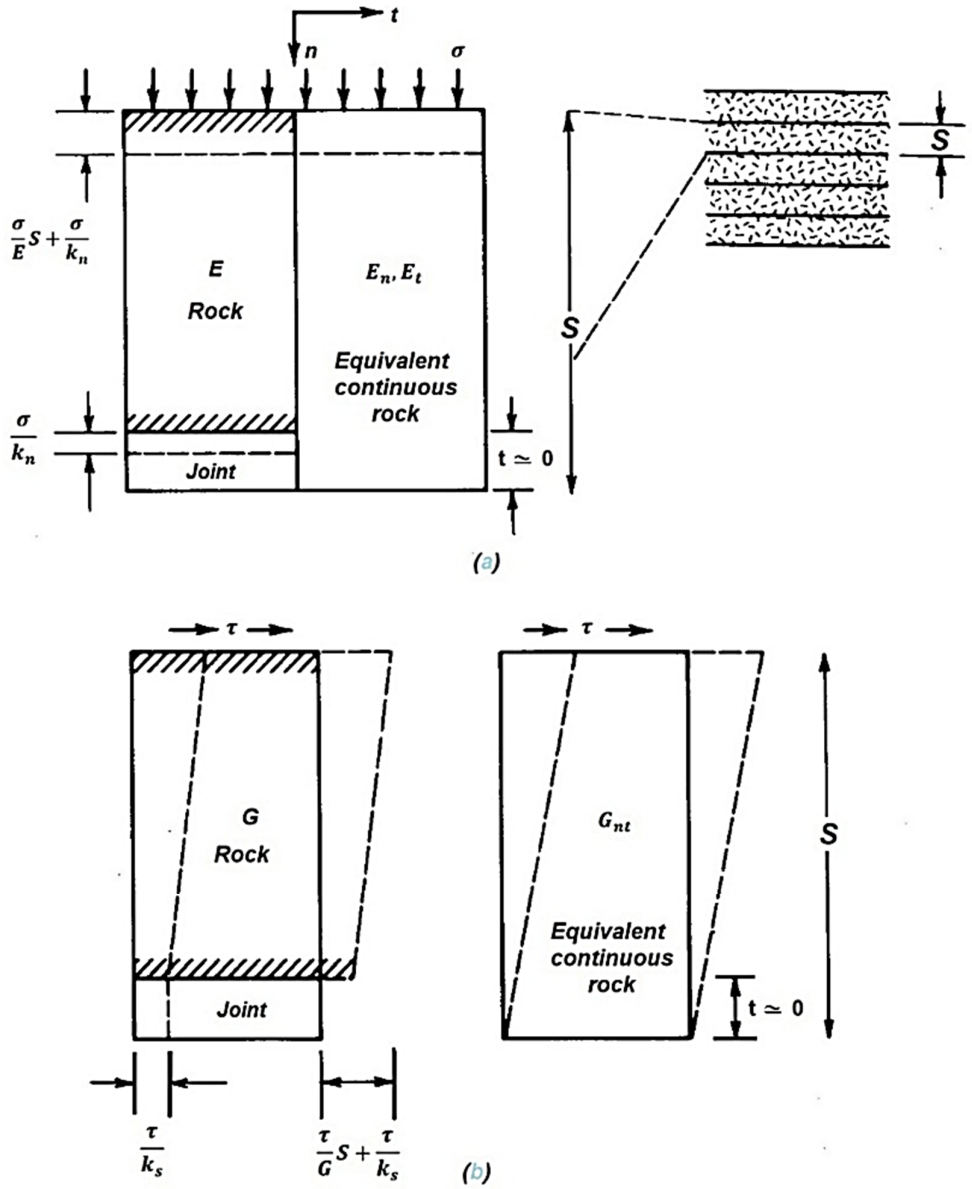

Figure 1 Represent an 'equivalent' transversely isotropic material with a regularly jointed rock (Goodman [36]).

Based on elasticity theory, the shear modulus can be calculated using Poisson's ratio and the modulus of elasticity (G=E/(2(1+ϑ)). Considering the limited changes in Poisson's ratio of medium-strength rock (0.2 -0.25), the effect of Poisson's ratio is neglected due to simplification and the G parameter removed from Equation (2-a). It is noticed that this assumption may not be true in some cases; however, Equation (2-a) is defined by:

$$D_f = f(E, k_s, k_n, S) \quad (2\text{–b})$$

In rock engineering projects in or on jointed rock mass, geometrical characteristics of discontinuities are generally not satisfied by the S factor. Rock engineers faced the inherent nature of rock mass heterogeneity as the greatest challenge to obtain D_f, and the empirical model considered to deal with it. However, a realistic prediction of D_f needs geometrical factor-related discontinuity considering the geometry, density, orientation, size, and number of joint set parameters. The authors suggested using the GSI index, which concentrates on describing rock structures and block surface conditions, instead of the S factor. GSI is widely utilized for estimating the rock mass strength and the rock mass deformation parameters; however, it practically has the most suitable adaptation to cover joint geometry; therefore, Equation (2-b) can be restated as follows:

$$D_f = f(E, k_s, k_n, GSI) \quad (3)$$

Furthermore, the deformation modulus is a ‘‘linking’’ parameter for the rock mass deformability behaviour derived by the applied stress and measured strain that includes the elastic and inelastic values of an in-situ rock mass [1]. On the one hand, Young’s modulus of intact rock, the normal and shear stiffness of the joint, and its spacing are the influential parameters affecting the modulus of deformation based on the analytical method; on the other hand, the intact rock and discontinuity, as the main components of rock mass are under the influence of in-situ stress, due to the Earth's crust, which has a predictable effect on E, k_s, and k_n. Logically, a reliable empirical model was not only dependable on deformability characteristics of intact rock and joint (set) but also relies on in-situ stress with geological processes during the rock mass formation. Other types of stress such as the thermal and physicochemical present in nuclear waste storage and hydrocarbon reservoirs, are outside the scope of this study. What is referred to as in-situ stress in civil projects is typically gravitational, tectonic, and induced stress [22].

As mentioned (Sec. 1), the corresponding deformation of the rock mass is measured by applying a specific load to a limited area of the rock mass in a borehole or gallery and then the D_f value align loading direction was calculated. Logically, not only the elastic modulus of intact rock but also the shear and normal stiffness of discontinuities are affected by the in-situ stress [8, 34, 14]. Consequently, a reliable predictive model to estimate D_f requires mechanical parameters of intact rock and joint, i.e. E_i, k_s, and k_n, respectively, the joint’s geometrical characteristics, i.e. GSI, and in-situ stress. So Equation (3) can be defined as follows:

$$D_f = f(E, k_s, k_n, GSI, \sigma_{rm}) \quad (4)$$

where σ_{rm} represents the in-situ stress corresponding to the desired deformation modulus direction. However, in-situ stress should theoretically be included in the empirical model, something that has not been considered so far.

3. Review of empirical models’ PIPs participation

In the last decades, many empirical models have been published with single or multiple input parameters or indices. In chronological order, the researchers used a simple index such as RQD, and then by introducing various rock mass classification indices such as RMR, Q, RMI, and GSI, the empirical models were developed by their participation. Then, other parameters, such as Young’s modulus and uniaxial compressive strength of intact rock, depth, and longitudinal ultrasonic wave velocity participated in the earlier models. Based on PIPs (Equation 4), the participation of the above parameters in the seventy empirical models was comprehensively evaluated (Table 2). The input parameters are categorized into three groups as follows:

- Where the input parameter is similar to the PIPs, it is indicated by the symbol (✓).
- If the input parameter has been equivalent to a principal parameter, it is shown by the symbol (≈). The equivalent parameters are derived from experimental equations such as RMR_{89}=GSI+5 and Q=$e^{(GSI-44)/9}$. Besides, in-situ stress ($\sigma_{rm} = f(\sigma_V, \sigma_H, \sigma_h)$) is a function of the gravitational (σ_V=ρgH) and tectonic (σ_H, σ_h) stresses; where ρ is rock density; H is the depth considering as an equivalent factor with in-situ stress. In

addition, there are experimental equations that correlate the E_i with UCS (E_i=MR×UCS), where "*MR*" was proposed by Hoek and Diederichs [12], as well as E_i with V_p (E_i=ρV_p^2) (Goodman [36]).

- The lack of the participial PIPs or their equivalents is denoted by the symbol (–).

Accordingly, in terms of statistical categorization, the principal parameters participation in seventy of the cited empirical models (Table 2) fall into three main classes, which are denoted by the directly exist, indirectly exist, and nonexistent, respectively (Figure 2).

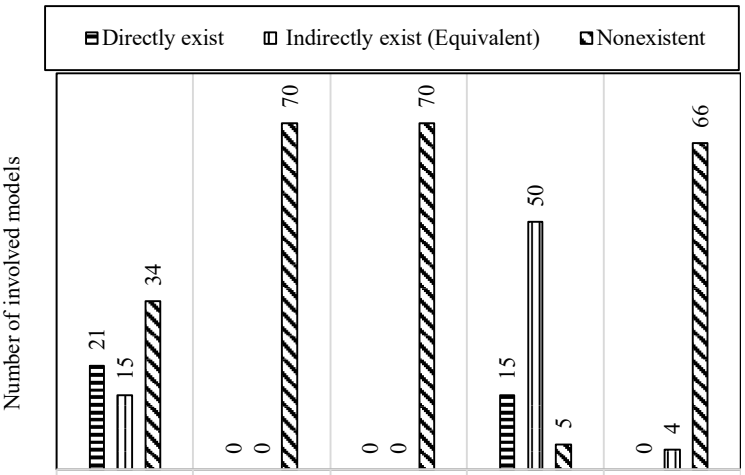

	Ei	ks	kn	GSI	σrm
Directly exist	21	0	0	15	0
Indirectly exist (Equivalent)	15	0	0	50	4
Nonexistent	34	70	70	5	66

Figure 2 The PIPs participation in seventy empirical models.

The participial PIPs in empirical equations (Table 2) are summarised as follows:

- The direct and indirect existence of E_i are 30% and 21%, respectively; in other words, only half of the models are participated in the E_i or its equivalent.
-
- The joint's shear and normal stiffness do not exist in any models; in other words, the joint's mechanical parameters haven't participated in models.

Table 2. The participation of E_i, K_s, K_n, GSI, and σ_{rm} in empirical models.

No.	References	Empirical model(s)	E_i	K_s	K_n	GSI	σ_{rm}	Descriptions
1	Coon and Merritt [37]	$E_d/E=0.0231RQD-1.32$; RQD(%) > 50	✓	–	–	≈	–	Dworshak dam site, Granite gneiss; Forks dam, gneiss; Yelloe tail dam, limestone; Glen Canyon dam, sandstone
2		$E_d/E=0.15$; RQD(%) < 50	✓	–	–	≈	–	
3	Bieniawski [9]	$E_d=10^{(RMR-20)/38}$; R^2 = 0.91	–	–	–	≈	–	for RQD(%) < 50
4	Bieniawski [38]	$E_d=2RMR-100$; 90 > RMR > 55	–	–	–	≈	–	With a prediction error of 18.2%; Based on 22 project data in the world; Rock mass types: siltstone, sandstone, mudstone, shale, dolerite, greywacke, and phyllite; The RMR system should not be applied to massive rock masses (Palmström, Singh, 2001).
5	Serafim and, Pereira [39]	$E_d=10^{(RMR-10)/40}$; for 55 > RMR > 30.	–	–	–	≈	–	Rock mass types: siltstone, sandstone, mudstone, shale, dolerite, granite, and gneiss. The RMR system should not be applied for massive rock masses (Palmström and Singh, 2001).
6	Gardner [40]	$E_m/E=0.0231\times RQD-1.32$ (≥0.15)	✓	–	–	≈	–	
7	Nicholson and Bieniawski [41]	$E_m=[E_l/100][0.0028RMR^2+0.9e^{(RMR/22.82)}$	✓	–	–	≈	–	Argillaceous and arenaceous rock; No. of data: 36
8	Grimstad and Barton [42]	$E_m=25\log Q$)	–	–	–	≈	–	The Q system should only be applied for very strong, massive rocks UCS > 150 MPa.
9	Mitri et al. [43]	$E_d=E_i[0.5(1-\cos(\pi RMR/100)]$	✓	–	–	≈	–	
10	Palmström [44]	$E_m=5.6\ RMi^{0.375}$	–	–	–	≈	–	For jointed rock mass, RMi > 0.1
11	Verman et al. [45]	$E_m=0.3H^{\alpha}10^{(RMR-20/38)}$; 0.16 < α < 0.3; H > 50 m	–	–	–	≈	≈	In-situ uniaxial compressive test in the poor and dry rock mass
12	Hoek and Brown [2]	$E_m=\sqrt{\frac{\sigma_{ci}}{100}}10^{(GSI-10/40)}$; σ_{ci}<100MPa	≈	–	–	✓	–	Rock type: slate, schist, phyllite, and weak rock
13	Palmström and Singh [46]	$E_m=7RMi^{0.4}$	–	–	–	≈	–	1 < RMi < 30; Limited accuracy for σ_c<100MPa
14	Hoek et al. [11]	$E_m=(1-D/2)\sqrt{\frac{\sigma_{ci}}{100}}10^{GSI-10/40}$	≈	–	–	✓	–	σ_{ci} < 100 MPa
15		$E_m=(1-D/2)\sqrt{\frac{\sigma_{ci}}{100}}10^{\frac{RMR-10}{40}}$	≈	–	–	≈	–	0 < D < 1
16	Barton [47]	$E_m=10\times(Q\frac{\sigma_c}{100})^{1/3}$	≈	–	–	≈	–	Rock type: schist, quartz, phyllite, dolomite, marble
17		$E_m=10\times10^{(V_p-3.5)/3}$	≈	–	–	–	–	
18	Gokceoglu et al. [10]	$E_M=0.1451e^{0.0654\ GSI}$; r=0.675	–	–	–	✓	–	One hundred fifteen data sets obtained from in-situ plate loading and dilatometer tests belong to 2 dams in Turkey; rock types consist of quartz–diorite, limestone, shale.
19		$E_M=0.0736e^{0.0755RMR}$; r=0.672	–	–	–	✓	–	
20		$E_m=0.001[(\frac{E_i}{UCS})(1+\frac{RQD}{100})/WD]^{1.5528}$; r=	✓	-	–	≈	–	
21	Kayabasi et al. [48]	$E_M=4.32-3.42WD+\left[0.19E_i(1+(\frac{RQD}{100}))\right]$	✓	–	–	≈	–	
22		$E_M=0.1423[E_i(1+(RQD/100)/WD]^{1.1747}$	✓	–	–	≈	–	The statistical studies, multiple regression analysis; 57 plate loading test data; rock type: quartz–diorite, limestone, and shale; a coefficient of correlation of 0.74
23	Zhang and Einstein [49]	$E_d=E_i(10^{0.0186RQD-1.91})$	✓	–	–	≈	–	Rock types: siltstone, mudstone, sandstone, shale, dolerite, granite, greywacke, limestone, gneiss, and granite gneiss
24	Ramamurthy [50]	$E_J=E_i\ exp[(RMR-100)/17.4]$	✓	–	–	≈	–	
25		$E_j=E_i exp(0.8625logQ-2.875)$	✓	–	–	≈	–	
26	Sonmez et al. [51]	$E_m=E_i(s^a)^{0.4}$	✓	–	–	✓	–	$s=\exp\left(\frac{GSI-100}{9-3D}\right)$; a=0.5 for GSI≥30; a=0.65-$\frac{GSI}{200}$ for GSI<30;
27	Galera et al. [52]	$E_d=147.28\ e^{(RMR-100)/24}-0.202.RMR$; r^2=0.765	–	–	–	≈	–	Rock types: Igneous ،metamorphic, carbonate & detritic sedimentary.
28		$E_d=e^{(RMR-10)/18}$; r^2=0.742	–	–	–	≈	–	
29		$E_d=0.0876.RMR$; r^2= 0.8; RMR ≥ 50	–	–	–	≈	–	

30		$E_d=0.0876.RMR+1.056(RMR-50)^2$; $r^2=0.8$;	–	–	–	≈	–	
31		$E_d=E_i.e^{(RMR-100)/36}$; $r^2=0.8$	✓	–	–	≈	–	
32	Chun et al. [53]	$E_d=0.3228.e^{(0.0485RMR)}$	–	–	–	≈	–	Igneous rock types; $R^2=0.36$
33	Sonmeza et al. [54]	$E_d=E_i 10^{((RMR-100)(100-RMR)/4000\times exp(-\frac{RMR}{100}))}$	✓	–	–	≈	–	No. of data: 36; Diverse rocks include greywacke and agglomerate
34	Hoek and Diederichs [12]	$E_m=100\left(\frac{(1-D/2)}{(1+e^{\frac{75+25D-GSI}{11}})}\right.$	–	–	–	✓	–	No. of data: 496; The rock types are igneous, sedimentary, and metamorphic, belonging to China and Taiwan, and in-situ tests comprise flat jack and plate tests; some data were obtained by back analysis.
35		$E_m=E_i(0.02+\frac{(1-D/2)}{1+e^{(\frac{60+15D-GSI}{11})}})$	✓	–	–	✓	–	Where information on the uniaxial compressive strength of the intact rock is available.
36	Givshad et al. [55]	$E_d=0.398(1.055)^{GSI}$	–	–	–	✓	–	The rock type is limestone, with mountain building morphology which has shale interbeds (Iran's Asmary formation); 700 dilatometer tests.
37		$E_d=0.151\ E_i^{0.582}(1.039)^{GSI}$	✓	–	–	✓	–	
38	Chun et al. [1]	$E_m=\frac{(5.992Depth^2+1.883UCS^4+4.851RQD^3+0.031JS^5+2399.530JC)}{10000}$	≈	–	–	≈	≈	A total of 61 data sets belong to road and railway construction sites in Korea. The E_m values were measured using pressure meter tests in most cases.
39	Beiki et al. [56]	$E_m=tan\left(\sqrt{1.56+\left(Ln(GSI)\right)^2}\right)\sqrt[3]{UCS}$	≈	–	–	✓	–	No. of data: 150; Rock types: shale, sandstone–quartzite, limestone, and marl–limestone with silica veins, sandstone, siltstone, and mudstone which belong to the 4 dam sites in Iran.
40		$E_m=tan\left(ln(GSI)\right)log(UCS)\sqrt[3]{RQD}$	≈	–	–	✓	–	
41	Mohammadi and Rahmannejad [57]	$E_m=0.0003RMR^3-0.0193RMR^2+0.3157\ RMR+3.4064$; $R^2=0.84$	≈	–	–	≈	–	No. of data: 42; Mixed rock types
42	Song et al. [33]	$D_f=0.02386V_p^{4.326}$	≈	–	–	–	–	
43	Shen et al. [58]	$E_m=110e^{-\left(\frac{(RMR-110)}{37}\right)^2}$	–	–	–	≈	–	Field data from Bieniawski (1978), Serafim and Pereira (1983), and Stephens and Banks (1989). These data are from high–quality tests and are commonly acknowledged as reliable data sources (Hoek and Diederichs, 2006).
44		$E_m=1.14E_i e^{-\left(\frac{(RMR-116)}{41}\right)^2}$	✓	–	–	≈	–	
45	Ajalloeian. and Mohammadi [59]	$E_m=9\times10^{-7}GSI^{4.303}$ $R^2=0.78$; RMSE=8.2	–	–	–	≈	–	The data belonged to Khersan II double–arch concrete dam and its hydroelectric powerhouse; the rock type is limestone; a set of 28 data from plate load tests; RMR, Q, and GSI were evaluated in the same area as that in which the plate load tests were performed; 60 < RQD < 100; 30 < GSI < 65; RMR < 70; 0 < Q < 50.
46		$E_m=3\times10^{-6}RQD^{3.587}$ RMSE=9.0; $R^2=0.75$	–	–	–	≈	–	
47		$E_m=0.043RMR^2-3.662RMR+83.37$ $R^2=0.82$; RMSE=6.1	–	–	–	≈	–	
48		$E_m=-0.016Q^2+1.581Q+0.961$ $R^2=0.84$; RMSE=4.8	–	–	–	≈	–	
49	Nejati et al. [60]	$E_m=0.1627\ RMR-5.0165$; $R^2=0.67$	–	–	–	≈	–	Sedimentary rock types; No. of data = 52
50		$E_{rm}=-7.192+0.06469\sigma_c+0.20481RQD+0.030974JS+0.38384JC+0.1716GW$; $R^2=0.84$	≈	–	–	≈	–	Rock types are conglomerate, cherty limestone, and interbedded mudstones and sandstone belonging to the Gotvand dam site in Iran; 8 plate jacking and 44 dilatometer tests.
51	Karaman et al. [61]	$E_m=Is_{(50)}10^{(0.01RQD-0.25)}$	–	–	–	≈	–	Thirty-seven samples consist of 24 igneous, 8 metamorphic, and 5 sedimentary samples from Turkey.
52	Alemdag et al. [62]	$E_m=0.00067RQD^2+0.00067RQD\sigma+(0.00067RQD\sigma+0.00067\sigma^2)/(RQD+99.5)$; $R^2=0.735$	–	–	–	≈	–	No. of data: 50; Well–bedded siltstones; pressure–meter tests at 12 boreholes with a total length of 50 m and maximum test depth was 5 meters; the RQD values vary between 11% and 98%, with a mean value of 61.1%; with a genetic programming approach.
53	Rezaei et al. [63]	$E_m=3.322e^{0.023RQD}$; $R^2=0.38$	–	–	–	≈	–	Twenty-eight plate jacking tests belong to the Khersan II project in Iran.
54		$E_m=1.639Q^{0.78}$; $R^2=0.69$	–	–	–	≈	–	
55		$E_m=1.2716e^{0.044RMR}$; $R^2=0.68$	–	–	–	≈	–	
56		$E_m=1.059e^{0.043GSI}$; $R^2=0.65$	–	–	–	✓	–	
57		$E_m=8.407RMi^{0.543}$; $R^2=0.67$	–	–	–	≈	–	
58		$E_m=1.23e^{0.026RQD}$; $R^2=0.35$	–	–	–	≈	–	Eighty-nine plate jacking tests belong to the Bakhtiari project in Iran.
59		$E_m=1.797Q^{0.905}$; $R^2=0.57$	–	–	–	≈	–	
60		$E_m=0.326e^{0.063RMR}$; $R^2=0.62$	–	–	–	≈	–	
61		$E_m=0.237e^{0.059GSI}$; $R^2=0.58$	–	–	–	✓	–	
62		$E_m=3.942RMi^{0.703}$; $R^2=0.66$	–	–	–	≈	–	

63	Ramamurthy [64]	$E_j/E_i = exp(-0.0115J_f)$	✓	–	–	≈	–	
64		$M_{rj}/M_{ri} = exp(-0.0035\ J_f)$	✓	–	–	≈	–	
65	Shen et al. [15]	$E_m=0.295V_p^{2.387}$; $E_m=0.299e^{0.812V_p}$	≈	–	–	–	–	Rock type: basalt; Loaded plate; Acoustic tests should be carried out before the deformation test.
66		$E_m=0.1V_p^{3.267}$; $E_m=0.269e^{0.852V_p}$	≈	–	–	–	–	Rock type: sandstone; Loaded plate; Acoustic tests should be carried out before the deformation test
67	Radovanovic et al. [65]	$Em = -40.194 + 0.7p\ ln(Vp) - 5.168ln(Vp) - 0.030p^2 - 5.765p$	≈	–	–	–	≈	
68	Slavko et al. [66]	$E_m=0.059e^{0.0736(GSI+27z)} + (E_i GSI/600)(27z)^{0.1}$	✓	–	–	✓	≈	Data gathered from Verman et al.(1997) [45] and Cai et al. (2004) [67]
69	Shahverdiloo & Zare [13]	$D_{fn}=5.26\times10^{-6}(E_l)^{0.9979}\times B_n^{1.9979}\times RQD$; $R^2=0.8$	✓	–	–	≈	–	17 dilatometer tests belong to three hydropower projects in Iran
70	Hua et al. [8]	$E_m=(0.011+0.15Q)V_p^{2.5}$; $R^2=0.7$	≈	–	–	≈	–	84 plate bearing tests and geotechnical data sets belong to a hydropower station in the metamorphic rock (marble and slate with a small amount of lamprophyre dike), and the crustal stress is high in the rock mass.

Description:
B_n: Stress factor in dilatometer test; D: Disturbance factor; Di: Dilatometer test; D_{fn}: Deformation modulus of dilatometer test cycles (generally n= 1, 2, or 3); E_r, E, E_l or E_i: Elastic / Young's modulus of intact rock (GPa); E_{mass}, E_{rm}, E_M, E_j, D_f, or E_d: Rock mass Deformation modulus (GPa); g: Gravity acceleration; GW: ground water index; Is(50): Point load index; Jointed rock mass (index); J_n: Rating for the number of joint sets; J_f: Joint factor ($J_f = J_n/(n.r)$); JC: Joint condition; H or Z: Depth (meter); JS: Joint spacing; JRC: Joint roughness coefficient; M_{ri}: Modulus ratio of intact rock; M_{rj}: Modulus ratio of rock mass; MR, M: The modulus ratio (E/σ_{ci}); n: joint inclination coefficient; *n*: Corresponding parameter of slip plane angle with major principal stress direction; p: Pressure in MPa; *p*: the pressure in the rock mass obtained from in-situ test; PJT: Plate jacking test; Q̀: Modified tunnelling quality index: ($RQD/J_n \times J_r/J_a$); q_{ci}; σ_{ci}; UCS: Uniaxial compressive strength of intact rock (MPa); *r*: coefficient of regression; r: a parameter for the strength of the joint and is related to the joint fill; Q_c: Rock mass quality rating (Q normalized by σ_{ci} /100); RMR76: Rock mass rating 1976 version; RMR89: Rock mass rating 1989 version; s: Hoek and Brown criteria's constant; R^2or r^2: Determination coefficient; Vp, V_{ps}: seismic wave velocity in km/s; WD: Weathering degree; σ : Pressure meter test value; ρ: Rock density.

- The direct and indirect existence of GSI is about 21.5% and 71.5%, respectively. There are equivalent indices such as RMR and Q, or discontinuity's distance factor which indirectly represent GSI. However, the GSI's nonexistent part is less than 7%. Accordingly, joint geometrical factors have actively participated in pre-existing empirical models.
- The in-situ stress doesn't have any direct participation however indirect existence is about 6%. The depth factor has been directly related to gravitational stress, but the main horizontal in-situ stresses haven't participated in the pre-existing models.

4. Discussion

The analytical background of PIPs and the appropriate quantity and quality of input data lead to a more reliable predictive model. The deformation modulus directional nature is the most challenging aspect depending on the in-situ stress, geometrical characteristic of discontinuity, and mechanical characteristic of intact rock and discontinuity. Regardless of the limiting factors in terms of the analyzing method, which is mainly the conventional regression method, and the number of data, the main undeniable challenge facing empirical models is a lack of PIPs. The participation in seventy pre-existing empirical models (Table 2) is summarised as follows:

- Only one principal / equivalent parameter or index has participated in thirty-nine empirical models. Besides, two PIPs in twenty-nine models and three PIPs in only two models have participated, but there are no models with all PIPs (Figure 3).
- GSI is the only principal input parameter in Gokceoglu et al. [10], Hoek and Diederichs [12], Givshad et al. [55], and Rezaei et al. [63] empirical models.
- The GSI and E_i have directly participated in Givshad et al. [55], Hoek and Diederichs [12], and Sonmez et al. [51] empirical models. Moreover, the empirical models of Coon and Merritt [37], Galera et al. [52], Gardner [40], Gokceoglua et al. [10], Kayabasi et al. [48], Mitri et al. [43], Nicholson and Bieniawski [41], Ramamurthy [50], Shahverdiloo and Zare [13], Shen et al. [58], Sonmez et al. [35], and Verman et al. [45] involved an equivalent such as RMR, Q, RQD, or Jf instead of GSI along with E_i. In addition, Beiki et al. [56] and Hoek et al. [11] mentioned empirical models that substituted UCS for E_i, along with GSI.
- Not only in-situ stress indirectly with the depth factor but also GSI and E_i parameters directly participated in the models of Slavko et al. [66]. Besides, the model of Chun et al. [1] indirectly involved E_i, GSI, and σ_{rm}.
- The properties of intact rock and discontinuity were influential in the velocity of ultrasonic waves through the rock mass. The effect of each parameter on the wave velocity is followed to quantify the qualitative factors of discontinuity. Although the velocity of ultrasonic waves in a rock mass has a conceptual relationship with the characteristics of discontinuities, there is not a mathematical/analytical relationship to support the effect of longitudinal wave velocity (V_p) with PIPs, except Young's modulus of intact rock. Based on existing equations [36], the V_p is considered as an equivalent factor with E_i for empirical models of Barton [47], Song et al. [33], Shen et al. [15], Radovanovic et al. [65], and Hua et al. [8] (Table 2)

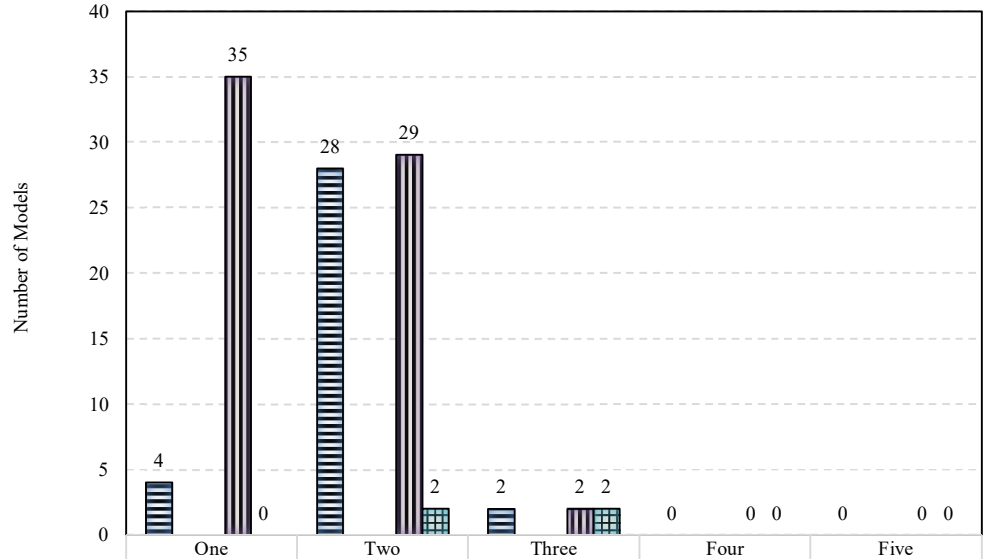

	One	Two	Three	Four	Five
Ei	4	28	2	0	0
ks	0	0	0	0	0
kn	0	0	0	0	0
GSI	35	29	2	0	0
In situ stress	0	2	2	0	0

Figure 3 The categorized models in ascending order of participated input parameters based on PIPs.

Due to the in-situ stress tensorial form, combining the in-situ stress effect with the mechanical parameters of PIPs leads to the empirical models with the desired simplification. Accordingly, Young's modulus of intact rock is replaced with the confined Young's modulus. In addition, the joint shear and normal stiffness are replaced by scaled stiffness due to certain normal stress. The mentioned confining pressure and normal stress are determined by the in-situ stress based on mathematical or numerical approaches. Shahverdiloo and Zare [34, 14] mentioned Young's modulus and joint stiffness were dependent on peripheral stresses. Moreover, the in-situ stress can be estimated or determined at a depth and alignment corresponding to the desired deformation modulus direction. However, the confined pressure around the intact rock and the normal stress on the discontinuity are determined by mathematical or numerical modelling. Confined Young's modulus (E_{ic}), scaled normal (k_{nn}) and shear (k_{sn}) stiffness can be determined with the laboratory triaxial and direct shear tests, respectively, or by applying the experimental equations. Authors such as Shahverdiloo and Zare [34, 14] mentioned the models which determined the aforementioned parameters as follows:

$$E_{ic}=E_i \times 2.42\, exp\left(-0.16\times\left(\frac{\sigma_3}{UCS}\right)^{-1}\right)+1 \quad (5)$$

$$k_{sn}=a.\sigma_n^b \quad (6\text{-a})$$

$$k_{nn}=c.e^{d.\sigma_n} \quad (6\text{-b})$$

where σ_3 is peripheral pressure in a triaxial test; σ_n is constant normal stress in a direct shear test; "a" is a coefficient in the range of 0.4482 to 1.6788, and "b" is a coefficient in the range of 0.4533 to 1.1622; the coefficients c & d are in the range of 2.55 to 2.59 and 0.261 to 0.321, respectively.

The gap of knowledge in existing empirical models has led to ignoring the effect of in-situ stress, which can be considered by replacing confined Young's modulus and scaled normal and shear joint stiffness with Young's modulus and normal and shear stiffness, respectively. Thus, the in-situ stress effect combined with mechanical principal input parameters and Equation (4) can be expressed as follows:

$$D_f = f(E_{ic}, k_{sn}, k_{nn}, GSI) \quad (7)$$

As mentioned (Sec. 1), deformation modulus is a directional parameter combining elastic and inelastic deformability components. The effect of peripheral stress on Young's modulus and joint stiffness has been confirmed by lab studies however the deformation modulus is affected by in-situ stress. Moreover, ultrasonic waves in the laboratory or field are a non-destructive method

used for measuring the velocity of longitudinal and transverse waves to calculate the dynamic modulus of elasticity, which is related to the static elastic modulus in the rock core sample or the in-situ rock mass. Besides, the near-surface of the earth has been the subject of studies, which resulted in several empirical models for estimating the modulus of deformation. Generally, ultrasonic tests deal with oil wells and reservoirs, deep mines, and infrequently in near-earth surface civil projects. The deformation modulus prediction with ultrasonic approaches comparatively is limited, i.e. the models of Barton [47]; Song et al. [33]; Shen et al. [15]; Radovanovic et al. [65]; Hua et al. [8] (Table 2). It seems down-hole test (Daraei et al. [68]) studies along with the development of mathematical and numerical modelling are necessary to obtain an empirical model for estimating reliable D_f.

5. Conclusions

The deformation modulus is a crucial input parameter in numerical and analytical deformability analysis. The weak participation of principal parameters is an inevitable consequence of poor reliability in diverse empirical models for predicting rock mass deformation modulus. This study develops the theoretical dimension of the deformation modulus empirical model. The presented conceptual framework is supported by analytical methods with an emphasis on in-situ stress. The main achievements are defined as follows:

- Young's modulus of intact rock, the joint's shear and normal stiffness, the joint set spacing, and in-situ stress are analytical base parameters that are directly related to a rock mass deformation modulus. The GSI practically can be replaced with the joint set spacing factor due to considering the geometry, density, orientation, size, and number of joint set parameters.
- Among seventy empirical models (Table 2), the total number of models with the direct or indirect participation of E_i, k_s, k_n, GSI, and σ_{rm} are 36, 0, 0, 65, and 4, respectively. In other words, joint stiffness has any, but GSI has a major (92.8%) participation in earlier models. Besides, in-situ stress has a minor (5.7%), but Young's modulus has a moderate participation (51.4%).
- Due to the tensorial form of in-situ stress and its impact on D_f, practically, it was considered the replacement parameters as E_{ic}, k_{ns}, and k_{nn} [34, 14] instead of E_i, k_n, k_s and in-situ stress. The specified confining pressures and normal stress on laboratory specimens are achieved by mathematical or numerical approach.
- The E_{ic}, k_{ns}, and k_{nn} [34, 14] are replaced with E_i, k_n, and k_s, respectively, to consider the tensorial form of in-situ stress impact on D_f while maintaining the simplicity of the empirical model. The specified confining pressures in the triaxial test and normal stress on the shear test are achieved by mathematical or numerical approach.

This study develops a conceptual framework as the first step in making the process of an empirical model. There is a need for further research in terms of the analysis approach and validation of the PIPs. Besides, it is possible to draw the attention of researchers to modelling not only civil but also oil and deep mine engineering projects with numerical approaches to evaluate the sensitivity of the deformation behaviour of rock mass based on a mechanical parameter that is affected by the in-situ stress regime.

References

[1]. Chun, B.S., Ryu, W.R., Sagong, M., and Do, J.N. (2009). Indirect estimation of the rock deformation modulus based on polynomial and multiple regression analyses of the RMR system. *International Journal of Rock Mechanics and Mining Sciences*, 46, 649–658.

[2]. Hoek, E., & Brown, E.T. (1997). Practical estimates of rock mass strength. *International Journal of Rock Mechanics and Mining Sciences*, 34(8), 1165-1186.

[3]. Menard, L. (1975). The Menard pressuremeter: Interpretation and application of the pressuremeter test results to foundations design. *Sols Soils*, 26, 5–43.

[4]. Wittke, W. (2014). Rock mechanics based on an anisotropic jointed rock model (AJRM), John Wiley & Sons, Part C, Chp. 15, 57 P.

[5]. Goodman, R.E., Van, T.K., and Heuze, F.E. (1968). Measurement of rock deformability in boreholes. The 10th United States Symposium on Rock Mechanics (USRMS). OnePetro, Austin, May, 20–22.

[6]. Aksoy, C.O., Geniş, M., Aldaş, G.U., Özacar, V., Özer, S.C., and Yılmaz, Ö. (2012). A comparative study of the determination of rock mass deformation modulus by using different empirical approaches. *Engineering Geology*, 131, 19–28.

[7]. Hashemi, M., Moghaddas, S., and Ajalloeian, R. (2010). Application of rock mass characterization for determining the mechanical properties of rock mass: a comparative study. *Rock Mechanics and Rock Engineering*, 43, 305–320.

[8]. Hua, D., Jiang, Q., Liu, R., Gao, Y., and Yu, M. (2021). Rock mass deformation modulus estimation models based on in-situ tests. *Rock Mechanics and Rock Engineering*, 54, 5683–5702.

[9] Bieniawski, Z.T. (1974). Engineering classification of jointed rock masses. *International Journal of Rock Mechanics and Mining Sciences & Geomechanics Abstracts*, Pergamon, 11, 244.

[10]. Gokceoglua, C., Sonmeza, H., and Kayabasib, A. (2003). Predicting the deformation moduli of rock masses. *International Journal of Rock Mechanics and Mining Sciences*, 40, 701–710.

[11]. Hoek, E., Carranza-Torres, C., & Corkum, B. (2002). Hoek-Brown failure criterion-2002 edition. *Proceedings of NARMS-Tac*, *1*(1), 267-273.

[12]. Hoek, E. and Diederichs, M.S. (2006). Empirical estimation of rock mass modulus. *International Journal of Rock Mechanics and Mining Sciences*, 43, 203–215.

[13]. Shahverdiloo, M.R. and Zare, S. (2021b). A new correlation to predict rock mass deformability modulus considering loading level of dilatometer tests, *Geotechnical and Geological Engineering*, 39, 5517–5528.

[14]. Shahverdiloo, M.R. and Zare, S. (2023). Experimental study of normalized confining pressure effect on Young's modulus in different rock types. *Arabian Journal of Geosciences*, 16, 1–12.

[15]. Shen, X., Chen, M., Lu, W., and Li, L. (2017). Using P wave modulus to estimate the mechanical parameters of rock mass,. *Bulletin of Engineering Geology and Environment*, 76, 1461–1470.

[16]. Zhang, L. (2010). Method for estimating the deformability of heavily jointed rock masses. *Journal of Geotechnical and Geoenvironmental Engineering*, 136, 1242-1250.

[17]. Duncan, J.M. and Goodman, R.E. (1968). Finite element analysis of slopes in jointed rocks. U.S. Army Corps of Engineers Rep. TR No. 1-68, Washington, D.C.

[18]. Kulhawy, F.H. (1978). Geomechanical model for rock foundation settlement. *Journal of the Geotechnical Engineering Division*, 104, 211-227.

[19]. Chen, E.P. (1989). A constitutive model for jointed rock mass with orthogonal sets of joints, ASME Trans. *J. Appl. Mech*, 56, 25–32.

[20]. Amadei, B. (1983). Rock anisotropy and the theory of stress measurements, Lecture notes in engineering, C.A. Brebbia and S.A. Orszag, eds., Springer, Berlin, 478 P.

[21]. Amadei, B. and Savage, W.Z. (1993). Effect of joints on rock mass strength and deformability. Chapter 17 in Comprehensive Rock Engineering, 1, 331-365.

[22]. Huang, T.H., Chang, C.S., and Yang, Z.Y. (1995). Elastic moduli for fractured rock mass. *Rock Mechanics and Rock Engineering*, 28, 135-144.

[23]. Fossum, A.F. (1985). Effective elastic properties for a randomly jointed rock mass. *International Journal of Rock Mechanics and Mining Sciences & Geomechanics Abstracts*, 22, 467-470.

[24]. Gerrard, C.M. (1982). Elastic models of rock masses having one, two, and three sets of joints. *International Journal of Rock Mechanics and Mining Science & Geomechanics Abstracts*.

[25]. Oda, M (1988). An experimental study of the elasticity of mylonite rock with random cracks. *International Journal of Rock Mechanics and Mining Sciences & Geomechanics Abstract*. 25, 59–69.

[26]. Kulatilake, P. H., Wang, S., & Stephansson, O. (1993, October). Effect of finite size joints on the deformability of jointed rock in three dimensions. In *International journal of rock mechanics and mining sciences & geomechanics abstracts* (Vol. 30, No. 5, pp. 479-501). Pergamon.

[27] Cai, M., & Wang, X. (2015, May). A non-uniform velocity model and flac/specfem2d coupled numerical simulation of wave propagation in underground mines. In *ISRM Congress* (pp. ISRM-13CONGRESS). ISRM.

[28]. Cui, L., Sheng, Q., Zheng, J., Xie, M., and Liu, Y. (2022). A unified deterioration model for elastic modulus of rocks with coupling influence of plastic shear strain and confining stress. *Rock Mechanics and Rock Engineering*, 55, 7409–7420.

[29]. Hsieh, A., Dyskin, A.V., and Dight, P. (2014). The increase in Young's modulus of rocks under uniaxial compression. *International Journal of Rock Mechanics and Mining Sciences*, 70, 425–434.

[30]. Marinos, P. and Hoek, E. (2001), Estimating the geotechnical properties of heterogeneous rock masses such as flysch. *Bulletin of Engineering Geology and Environment*, 60, 85–92.

[31]. Yang, S.Q., Jing, H.W., Li, Y.S., and Han, L.J. (2011). Experimental investigation on mechanical behavior of coarse marble under six different loading paths. *Experimental Mechanics*, 51, 315–334.

[32]. Labrie, D., Conlon, B., Anderson, T., & Boyle, R. F. (2004). Measurement of in-situ deformability in hard rock. *Proceedings ISC-2 on Geotechnical and Geophysical Site Characterization, Porto, Portugal. Ed. Milpress*, 963-970.

[33]. Song, Y.H., Ju, G.H., and Sun, M. (2011). Relationship between wave velocity and deformation modulus of rock masses. *Rock and Soil Mechanics*, 32, 1507–1567.

[34]. Shahverdiloo, M.R. and Zare, S. (2021a). Studying the normal stress influential factor on rock

joint stiffness using CNL direct shear test. *Arabian Journal of Geosciences*, 14, 1–11.

[35]. Van, P., & Vásárhelyi, B. (2014). Sensitivity Analysis of GSI based Mechanical Characterization of Rock Mass. *Periodica Polytechnica, Civil Engineering*, *58*(4), 1-8.

[36]. Goodman, R.E. (1989). Introduction to Rock Mechanics (2^{nd} edition). New York, Wiley, 562 P.

[37]. Coon, R.F. and Merritt, A.T. (1970). Predicting in-situ modulus of deformation using rock quality indexes, Special Technical Publication No. 477. American Society for Testing Materials, Philadelphia.

[38]. Bieniawski, Z.T. (1978). Determining rock mass deformability: experience from case histories. *International Journal of Rock Mechanics and Mining Sciences & Geomechanics Abstracts*, 15, 237–247.

[39]. Serafim, J.L. and Pereira J.P. (1983). Consideration of the geomechanical classification of Bieniawski. In Proc. Int. Symposium on Engineering Geology and Underground Construction, Lisbon, Sep. 12–15, 1, 12.

[40]. Gardner, W.S. (1987). Design of drilled piers in Atlantic Piedmont. Foundations and excavations in decomposed rock of the Piedmont province, ASCE, Reston, 9, 62–86. https://cedb.asce.org/CEDBsearch/record.jsp?dockey=0051472.

[41]. Nicholson, G.A. and Bieniawski, Z.T. (1990). A nonlinear deformation modulus based on rock mass classification. *International Journal of Mining and Geological Engineering*, 8, 181–202.

[42]. Grimstad, E.D. and Barton, N. (1993). Updating the Q–system for NMT. In Proceedings of the International Symposium on Sprayed Concrete–Modern use of wet mix sprayed concrete for underground support Fagernes, Oct. 22–26, 46–66. https://www.scirp.org/(S(i43dyn45teexjx-455qlt3d2q))/reference/referencespapers.aspx?referenceid=2013391

[43]. Mitri, H.S., Edrissi, R., and Henning J.G. (1995). Finite–element modeling of cable–bolted stopes in hard–rock underground mines. Transactions–Society for Mining Metallurgy and Exploration Incorporated, 298: 1897–1902.

[44]. Palmström, A. (1996). Characterizing rock masses by the RMi for use in practical rock engineering, part 2: some practical applications of the rock mass index (RMi). *Tunnelling and. Underground Space Technology*, 11, 287–303.

[45]. Verman, M., Singh, B., Viladkar, M.N., and Jethwa, J.L. (1997). Effect of tunnel depth on the modulus of deformation of rock mass. *Rock Mechanics and Rock Engineering*, 30, 121–127.

[46]. Palmström, A. and Singh, R. (2001). The deformation modulus of rock masses—comparisons between in-situ tests and indirect estimates. *Tunnelling and Underground. Space Technology*, 16, 115–131.

[47]. Barton, N. (2002). Some new Q-value correlations to assist in site characterisation and tunnel design. *International Journal of Rock Mechanics and Mining Sciences*, 39, 185-216. doi.org/10.1016/S1365-1609(02)00011-4

[48]. Kayabasi, A., Gokceoglu, C.A.N.D.A.N., and Ercanoglu, M.U.R.A.T. (2003). Estimating the deformation modulus of rock masses: a comparative study. *International Journal of Rock Mechanics and Mining Sciences*, 40, 55–63. doi.org/10.1016/S1365-1609(02)00112-0.

[49]. Zhang, L. and Einstein, H.H. (2004). Using RQD to estimate the deformation modulus of rock masses. *International Journal of Rock Mechanics and Mining Sciences*, 41, 337–341. doi.org/10.1016/S1365–1609(03)00100–X.

[50]. Ramamurthy, T. (2004). A geo–engineering classification for rocks and rock masses. *International Journal of Rock Mechanics and Mining Sciences*. 41, 89–101.

[51]. Sonmez, H., Gokceoglu, C., and Ulusay, R. (2004). Indirect determination of the modulus of deformation of rock masses based on the GSI system. *International Journal of Rock Mechanics and Mining Sciences*, 41, 849–857.

[52]. Galera, J.M., Alvarez, M., and Bienawski Z.T. (2005). Evaluation of the deformation modulus of rock masses: Comparison by pressuremeter and dilatometer tests with RMR prediction. In: ISP5–PRESSIO 2005 International Symposium, 2, 239–256. https://subterra–ing.com/wp–

[53]. Chun, B.S., Lee, Y.J., and Jung S.H. (2006). The evaluation for estimation method of deformation modulus of rock mass using RMR system. *Journal of the Korean GEO–environmental Society*, 7, 25–32.

[54]. Sonmez, H., Gokceoglu, C., Nefeslioglu, H.A., and Kayabasi, A. (2006). Estimation of rock modulus: for intact rocks with an artificial neural network and for rock masses with a new empirical equation, *International Journal of Rock Mechanics and Mining Sciences*, 43, 224–235.

[55]. Givshad, A.D., Memarian, H., and Rezaei, F. (2008). Investigation on deformability modulus of asmary formation rock mass, by dilatometer tests. The International Society for Rock Mechanics–International Symposium–5th Asian Rock Mechanics Symposium, OnePetro, Tehran, Nov. 24–26,. 239–246.

[56]. Beiki, M., Bashari, A., and Majdi, A. (2010). Genetic programming approach for estimating the deformation modulus of rock mass using sensitivity

analysis by neural network. *International Journal of Rock Mechanics and Mining Sciences*, 47, 1091–1103.

[57]. Mohammadi, H. and Rahmannejad, R. (2010). The estimation of rock mass deformation modulus using regression and artificial neural networks analysis. *Arabian Journal of Sciences and Engineering*, 35, 205.

[58]. Shen, J., Karakus, M., and Xu, C.(2012). A comparative study for empirical equations in estimating deformation modulus of rock masses. *Tunnelling and Underground Space Technology*, 32, 245–250.

[59]. Ajalloeian, R. and Mohammadi, M. (2014). Estimation of limestone rock mass deformation modulus using empirical equations. Bulletin of Engineering Geology and Environment.

[60]. Nejati, H.R., Ghazvinian, A., Moosavi, S.A., and Sarfarazi, V. (2014). On the use of the RMR system for estimation of rock mass deformation modulus. *Bulletin of Engineering Geology and Environment*, 73, 531–540.

[61]. Karaman, K., Cihangir, F., and Kesimal, A. (2015). A comparative assessment of rock mass deformation modulus. *International Journal of Mining Sciences Technology*, 25, 735–740.

[62]. Alemdag, S., Gurocak, Z., Cevik, A., Cabalar, A.F., and Gokceoglu, C. (2016). Modeling deformation modulus of a stratified sedimentary rock mass using neural network, fuzzy inference, and genetic programming. *Engineering Geology*, 203, 70–82. doi.org/10.1016/j.enggeo.2015.12.-002.

[63]. Rezaei, M., Ghafoori, M., and Ajalloeian, R. (2016). Comparison between the in-situ tests' data and empirical equations for estimation of deformation modulus of rock mass. *Geosciences Research*, 1, 47–59.

[64]. Ramamurthy, T., Madhavi Latha, G., and Sitharam, T.G. (2016). Modulus ratio and joint factor concepts to predict rock mass response. *Rock Mechanics and Rock Engineering*, 50, 353–366.

[65]. Radovanović, S., Ranković, V., Anđelković, V., Divac, D., and Milivojević, N. (2018). Development of new models for the estimation of deformation moduli in rock masses based 3on in-situ measurements. *Bulletin of Engineering Geology and Environment*, 77, 1191–1202.

[66]. Slavko, T. and Veljko, L. (2019). A model for estimation of stress–dependent deformation modulus of rock mass. *International Journal of Mining and Geo–Engineering*, 53, 63–67.

[67]. Cai, M., Kaiser, P.K., Uno, H., Tasaka, Y., and Minami, M. (2004). Estimation of rock mass deformation modulus and strength of jointed hard rock masses using the GSI system. *International Journal of Rock Mechanics and Mining Sciences*, 41, 3–19.

[68]. Daraei, A., Sharifi, F., Qader, D. N., Hama Ali, H. F., and Kolivand, F. (2023). Prediction of the static elastic modulus of limestone using downhole seismic test in Asmari formation. *Acta Geophys*, 72, 247–255.

مشارکت پارامترهای تحلیلی در مدل‌های تخمینگر مدول تغییر شکل‌پذیری توده سنگ: مطالعه مروری

محمدرضا شاهوردیلو* و شکراله زارع

دانشکده مهندسی معدن، نفت و ژئوفیزیک ، دانشگاه صنعتی شاهرود، ایران

ارسال ۲۰۲۴/۰۳/۰۹، پذیرش ۲۰۲۴/۰۶/۱۰

* نویسنده مسئول مکاتبات: mr.shahverdiloo@shahroodut.ac.ir

چکیده:

مدول تغییر شکل‌پذیری توده‌سنگ برای آنالیز سازه‌های سنگی یک ضرورت است که عموما توسط مدل‌های تجربی با مشارکت یک تا پنج پارامتر/ شاخص پیش‌بینی می‌شود. بهرحال مشارکت مناسب پارامترهای ورودی برای تشکیل شالوده قابل اطمینان برای تخمین مدول تغییر شکل‌پذیری محل چالش بوده است. در این مطالعه، مفهوم پارامترهای اصلی ورودی برپایه روش تحلیلی (ریاضی) با تاکید بر تنش برجا توسعه داده شد. براساس مدل‌های ریاضی، مدول یانگ سنگ بکر، سختی‌های نرمال و برشی درزه، فاصله‌داری درزه و تنش برجا به عنوان پارامترهای اصلی تاثیرگذار معرفی شده‌اند. مروری بر هفتاد مدل تجربی قبلی نشان داد که بیشتر آنها با نقصان پارامترهای تحلیلی دست به گریبانند. با ملاحظه موضوعات اجرایی، شاخص مقاومت زمین‌شناسی (GSI) جایگزین فاکتور اصلی فاصله‌داری درزه شد. علاوه بر این، اثر تنش برجا بر مدول تغییر شکل پذیری با لحاظ تاثیر آن بر اجزای تشکیل دهنده توده‌سنگ یعنی سنگ بکر و درزه با استخراج مدول یانگ و سختی درزه به ترتیب تحت فشار محصورکننده و تنش نرمال مشخص در نظر گرفته شد. مشارکت همه پارامترهای اصلی تحلیلی و ملاحظات اجرایی می‌تواند اطمینان‌پذیری به مدل‌های تجربی را بهبود بخشیده تا با تخمین مدول‌های تغییرشکل‌پذیری مناسب، نتایج آنالیزهای عددی و تحلیلی تغییرشکل‌پذیری، از اطمینان بالاتری برخوردار شوند.

کلمات کلیدی: مدول تغییرشکل‌پذیری، پارامترهای تحلیلی، تنش برجا، سختی درزه، شاخص مقاومت زمین‌شناسی